

Supporting Information

Table S1. Parameters from Boltzmann Equation fits to GV data.

Boltzmann Coefficients		Offset		G/G _{max}		V _{1/2} (mV)		Slope (mV)			
Construct		mean	± sem	mean	± sem	mean	± sem	mean	± sem	n =	
SplHwt	No cNMP*	-0.013	± 0.016	0.033	± 0.021	-74	± 13	-38.3	± 34.8	11	
	cAMP	0.008	± 0.003	1	± 0	-67	± 2	-6.1	± 0.2	11	
	cGMP	-0.001	± 0.003	0.372	± 0.020	-71	± 1	-6.6	± 0.2	11	
SplHACterm	No cNMP	-0.015	± 0.006	1	± 0	-97	± 3	-6.6	± 0.7	4	
	359:360	No cNMP*	0.023	± 0.012	0.069	± 0.015	-33	± 4	-5.9	± 2.1	6
	1:1	cAMP	0.186	± 0.024	1	± 0	-38	± 3	-8.3	± 0.6	6
359:360	cGMP	0.069	± 0.020	0.414	± 0.075	-46	± 2	-10.1	± 0.8	6	
	No cNMP*	0.027	± 0.005	0.052	± 0.007	-19	± 12	-3.0	± 1.5	3	
	4:1	cAMP	0.187	± 0.003	1	± 0	-40	± 1	-9.0	± 0.1	3
359:363	cGMP	0.082	± 0.009	0.565	± 0.021	-50	± 1	-10.9	± 0.3	3	
	No cNMP*	0.009	± 0.015	0.035	± 0.007	-71	± 17	-9.0	± 5.2	4	
	cAMP	0.022	± 0.017	1	± 0	-66	± 1	-7.0	± 0.5	4	
355:360	cGMP	0.015	± 0.015	0.362	± 0.045	-80	± 1	-8.0	± 0.6	4	
	No cNMP			0.030	± 0.001					3	
	cAMP			0.959	± 0.013					3	
350:360	cGMP			0.211	± 0.049					3	
	No cNMP			0.056	± 0.011					3	
	cAMP			0.942	± 0.037					3	
350:363	cGMP			0.283	± 0.016					3	
	No cNMP			0.210	± 0.046					5	
	cAMP			0.958	± 0.011					5	
350:367	cGMP			0.490	± 0.063					5	
	No cNMP			0.685	± 0.043					3	
	cAMP			0.979	± 0.007					3	
359:367	cGMP			0.893	± 0.007					3	
	No cNMP	0.265	± 0.034	0.515	± 0.051	-79	± 4	-8.8	± 0.4	7	
	1:1	cAMP	0.780	± 0.021	1	± 0	-54	± 2	-11.8	± 0.7	7
359:367	cGMP	0.488	± 0.039	0.874	± 0.030	-69	± 3	-9.2	± 0.6	7	
	No cNMP	0.196	± 0.024	0.366	± 0.019	-85	± 4	-7.7	± 0.9	3	
	4:1	cAMP	0.740	± 0.008	1	± 0	-59	± 4	-13.9	± 1.4	3
A4	cGMP	0.423	± 0.014	0.852	± 0.006	-72	± 4	-10.9	± 0.7	3	
	No cNMP‡	0.034	± 0.016			-48	± 6	6.8	± 0.4	3	
	No cNMP‡	0.014	± 0.007			-73	± 8	-15.4	± 5.0	3	
	cAMP	0.090	± 0.019	1	± 0	-40	± 4	-6.9	± 0.5	3	
	cGMP ‡	0.274	± 0.003			-59	± 4	6.8	± 1.1	3	
A6	cGMP ‡	0.047	± 0.011			-61	± 3	-9.5	± 2.9	3	
	No cNMP‡	0.232	± 0.049			-62	± 8	11.3	± 0.7	3	
	No cNMP‡	0.336	± 0.020			-34	± 3	-17.3	± 2.4	3	
	cAMP	0.469	± 0.027	1	± 0	-3	± 7	-16.0	± 2.4	3	
R350A	cGMP	0.333	± 0.004	0.906	± 0.019	-23	± 5	-12.9	± 1.6	3	
	No cNMP‡	0.012	± 0.017			11	± 5	11.5	± 1.0	3	
	No cNMP‡	0.006	± 0.001			-11	± 9	-11.4	± 1.2	3	
	cAMP	0.079	± 0.013	1	± 0	-6	± 7	-10.2	± 13.7	3	
F351A	cGMP	0.079	± 0.008	0.317	± 0.048	-19	± 7	0.5	± 2.6	3	
	No cNMP*	0.023	± 0.002			93	± 75	47.5	± 17.6	3	
	No cNMP‡*	0.013	± 0.010			-71	± 3	-3.7	± 0.3	3	
	cAMP	0.011	± 0.001	1	± 0	-81	± 1	-6.7	± -6.0	3	
Q354A	cGMP	0.005	± 0.003	0.005	± 0.029	-80	± 1	0.2	± 0.3	3	
	No cNMP*	0.002	± 0.001	0.035	± 0.005	-62	± 3	-7.2	± 1.6	3	
	cAMP	0.012	± 0.005	1	± 0	-65	± 1	-6.5	± 0.7	3	
	cGMP	0.004	± 0.003	0.262	± 0.043	-70	± 1	-7.8	± 1.5	3	
W355A	No cNMP*	0.008	± 0.012	0.011	± 0.001	-190	± 171	-135.3	± 134.7	3	
	cAMP	0.026	± 0.004	1	± 0	-40	± 2	-5.2	± 0.5	3	
	cGMP*	0.006	± 0.021	0.061	± 0.012	-25	± 4	-7.0	± 6.1	3	
E356A	No cNMP‡	0.081	± 0.015			-52	± 4	8.9	± 3.6	3	
	No cNMP‡	0.028	± 0.003			-67	± 3	-7.0	± 2.6	3	
	cAMP	0.104	± 0.021	1	± 0	-47	± 1	-8.2	± 0.3	3	
	cGMP	0.047	± 0.008	0.555	± 0.058	-64	± 1	-6.9	± 0.3	3	
R367A	No cNMP	0.051	± 0.008	0.880	± 0.018	-70	± 3	-7.7	± 1.5	3	
	cAMP	0.058	± 0.009	1	± 0	-63	± 3	-8.1	± 0.4	3	
	cGMP	0.051	± 0.012	1.024	± 0.009	-69	± 2	-6.8	± 0.7	3	
D471A	No cNMP	0.011	± 0.006	0.451	± 0.051	-64	± 2	-6.9	± 0.4	3	
	cAMP	0.016	± 0.004	1	± 0	-59	± 1	-6.5	± 0.6	3	
	cGMP	0.013	± 0.003	0.991	± 0.043	-68	± 1	-6.8	± 0.6	3	
ΔQWE	No cNMP			0.572	± 0.039					5	
	cAMP			0.970	± 0.008					5	
	cGMP			0.872	± 0.029					3	
ΔQAF	No cNMP	0.319	± 0.029	0.650	± 0.038	-37	± 2	7.7	± 0.5	5	
	cAMP			1	± 0					5	

Data shown as mean ± s.e.m. * not well determined. ‡ product of two Boltzmann eqn.

Supplemental figures:

Fig. S1. Sequence alignment of the S4-S5 regions of several HCN and related channels.

HCN1, human NM_021072.3; HCN2, human NM_001194.3; HCN2, human NM_020897.2; HCN4, human NM_005477.2; HCN1, mouse NM_010408.3; HCH2, mouse NM_008226.2; SpHCN, invertebrate NM_214564.1; CNGA1, bovine 1.NM_174278.2; Tax4, C. elegans NM_066632.4; EAG1, mouse NM_001038607.2; EAG, rat 1.NM_031742.1; ERG, human NM_172057.2; Kv1.2, rat NM_023954.1

Fig. S2. SpHCN_{WT} current families recorded in the absence and presence of ligand along with block by ZD7288, an HCN channel specific blocker.

(A-D) SpHCN_{WT} currents measured (A), in the absence of ligand, (B) presence of 1 mM cGMP, (C) 1 mM cAMP, and (D) 1 mM cAMP + 100 µM ZD7288 in response to test voltage steps from -20 mV and -120 mV in increments of -10 mV followed by a voltage step to +40 mV. (E) SpHCN_{WT} currents measured during voltage steps to -100 and +100 mV as ZD7288 was applied to inside of patch. (F) Normalized current amplitudes measured at the end of the -100 mV pulse first in 1 mM cAMP (red bar) then in 1 mM cAMP + 100 µM ZD7288 (black bar). The data were fit by a single exponential with tau = 5.7 s.

Fig. S3. Functional split channels require co-expression of both VSD and PD, and reduced VSD-PD coupling is not a property of the VSD:PD ratio.

Oocytes were injected with different ratios of VSD:PD cRNAs: 4:1, 1:1, 0:1. (A) ZD-subtracted currents from split spHCN_(359:360) channels with a break in the S4-S5 linker, (B) ZD-subtracted currents from split spHCN_(359:367) channels with the S4-S5 linker + S5_{N-term} region deleted. (C) GV curves from split spHCN_(359:360) channels with cRNA ratios 4:1 (open symbols) and 1:1 (filled symbols). (D) GV curves from split spHCN_(359:367) channels.

Fig. S4. Simple 4 state model for closed state inactivation.

- (A) Model showing closed (C_0 , C_1), open (O), and inactivated (I) states with equilibrium constants $H(V)$, L , and J .
- (B) Po vs voltage plot shows activation without inactivation (red, $J = 0$), activation with voltage-independent inactivation (black, dashed, $J = 200$), and activation with voltage-dependent inactivation (black, solid, $J(V) = 0.1 * e^{(-V/8)}$). For all traces, $H(V) = 10^{-6}e^{(-V/8)}$ and $L = 100$).

Fig. S5. A simple state diagram which corresponds to the HA model shown in Fig. 2A.

State diagram shows how the equilibrium constants, H , K , and L , with coupling factors F , C , and E explicitly affect specific transitions.

Fig. S1

	S4	RYXXQWEXXF	S5
HCN1, human	(253)	ALRIVRFTKILSLLRLLSRLIRYIHQWEEIFHMTYDLASAVRIFNLIGMMLLCHWDGCLQFLVPLLQ	
HCN2, human	(323)	ALRIVRFTKILSLLRLLSRLIRYIHQWEEIFHMTYDLASAVMRICNLISMMLLCHWDGCLQFLVPMLQ	
HCN3, human	(206)	ALRIVRFTKILSLLRLLSRLIRYIHQWEEIFHMTYDLASAVRIFNLIGMMLLCHWDGCLQFLVPMQLQ	
HCN4, human	(373)	ALRIVRFTKILSLLRLLSRLIRYIHQWEEIFHMTYDLASAVVRIVNLIGMMLLCHWDGCLQFLVPMQLQ	
HCN1, mouse	(242)	ALRIVRFTKILSLLRLLSRLIRYIHQWEEIFHMTYDLASAVRIFNLIGMMLLCHWDGCLQFLVPLLQ	
HCN2, mouse	(296)	ALRIVRFTKILSLLRLLSRLIRYIHQWEEIFHMTYDLASAVMRICNLISMMLLCHWDGCLQFLVPMLQ	
SpHCN, urchin	(327)	ALKILRFAKLLSLLRLSRLMRFVSQWEQAF---NVANAVIRICNLVCMMLLIGHWNGLQYLVPMQLQ	
CNG1, bovine	(259)	-IKFGWNYPEIRLNRLLRISRMFEFFQRTET-----RTNYPNIFRISNLVMYIIIIHWNA CYSISKAI	
Tax-4, <i>C.elegans</i>	(278)	---WRGLPILRLNRLIRYKRVRNCLERTET-----RSSMPNAFRVVVVVWYIVIIIIHWNA CLYFWISEWI	
EAG1, mouse	(343)	SQGISSLFSSLKVVRLLRLGRVARKLDHYI-----EYGAAVLVLLVCVFGLA HWMACIWYSIGDYE	
EAG1, rat	(320)	---SSLFSSLKVVRLLRLGRVARKLDHYI-----EYGAAVLVLLVCVFGLA HWMACIWYSIGDYE	
ERG1, human	(523)	-----LLKTARLLRLVRVARKLDRYS-----EYGAAVLFLLMCTFALIAHWLACI WYAIGNME	
Kv1.2, rat	(138)	VLQFQNVRVVQIFRIMRILRIFKLSRHSK-GLQILGQTLKASMRELGLLI FFLFIGVILFSSAVYFAEAD	

Fig. S2

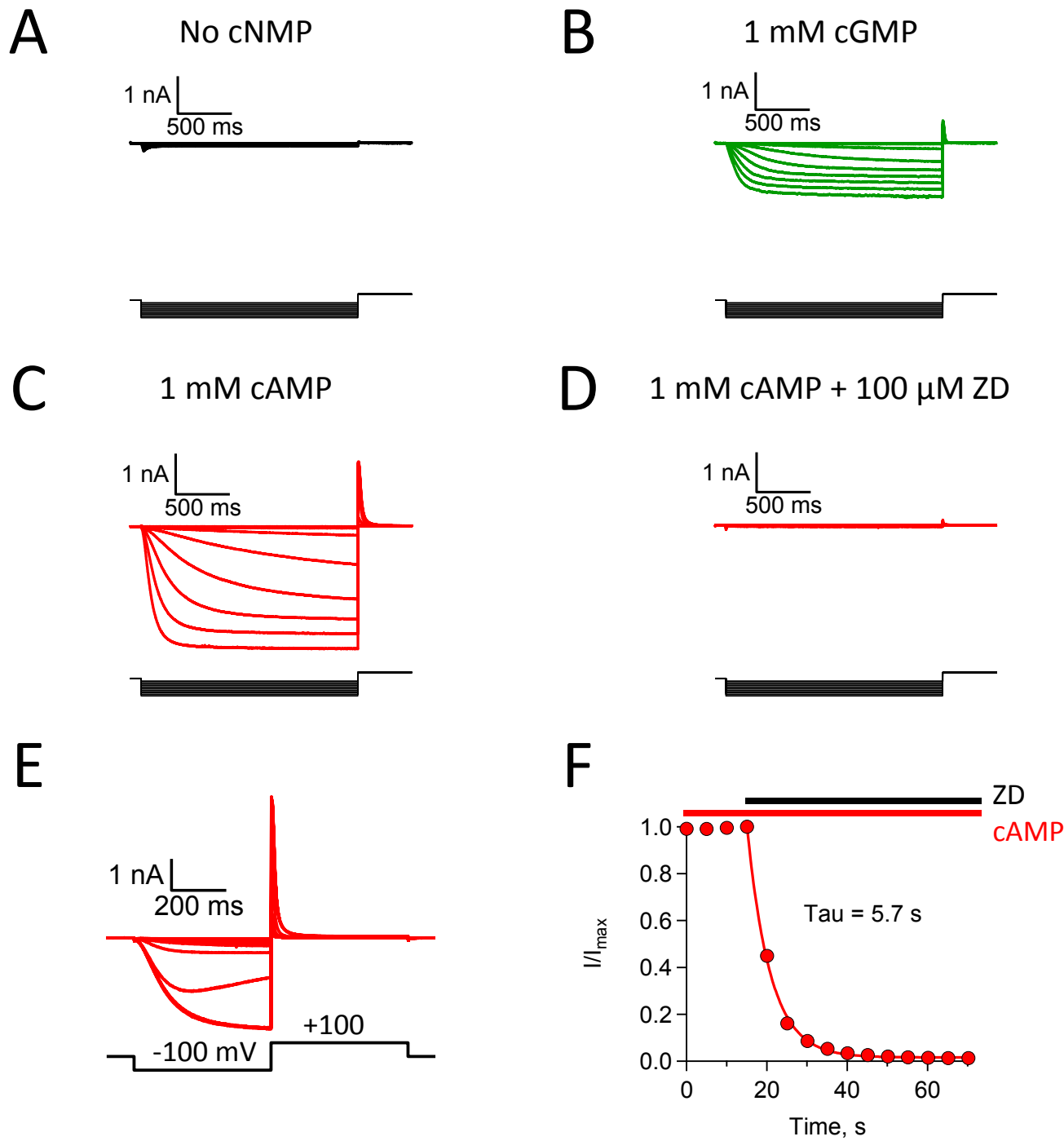


Fig. S3

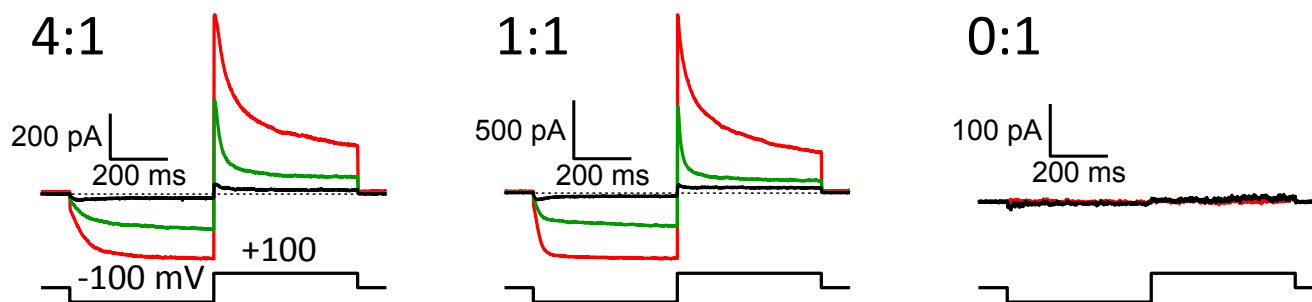
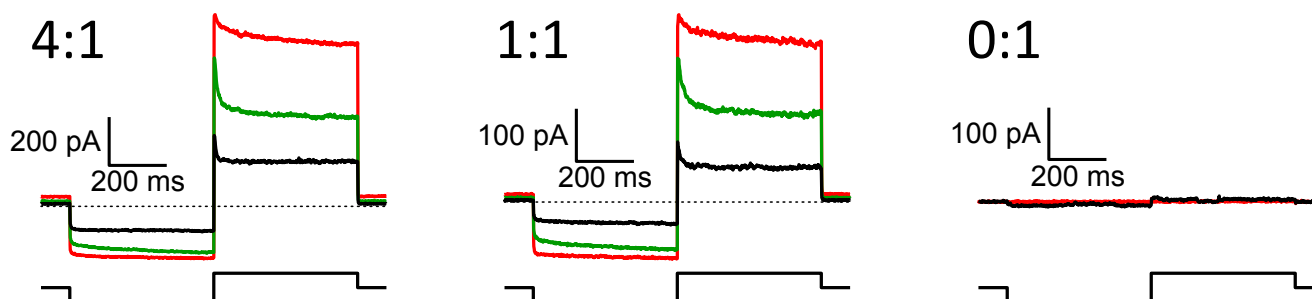
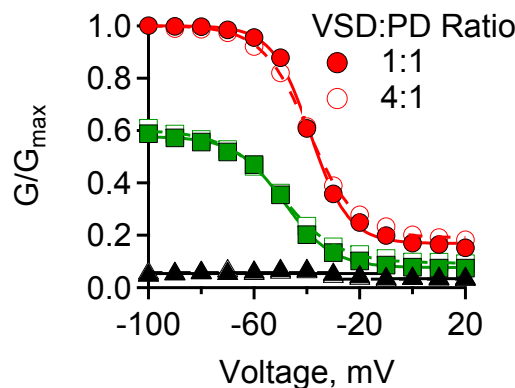
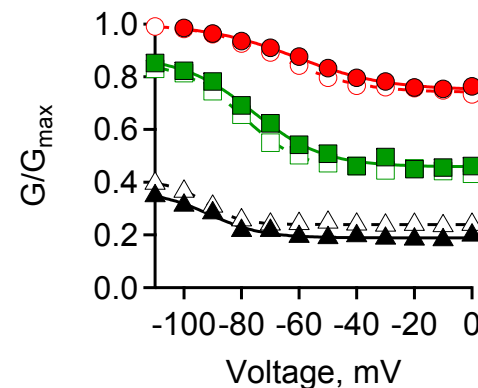
A*spHCN*_(359:360)**B***spHCN*_(359:367)**C** *spHCN*_(359:360)**D** *spHCN*_(359:367)

Fig. S4

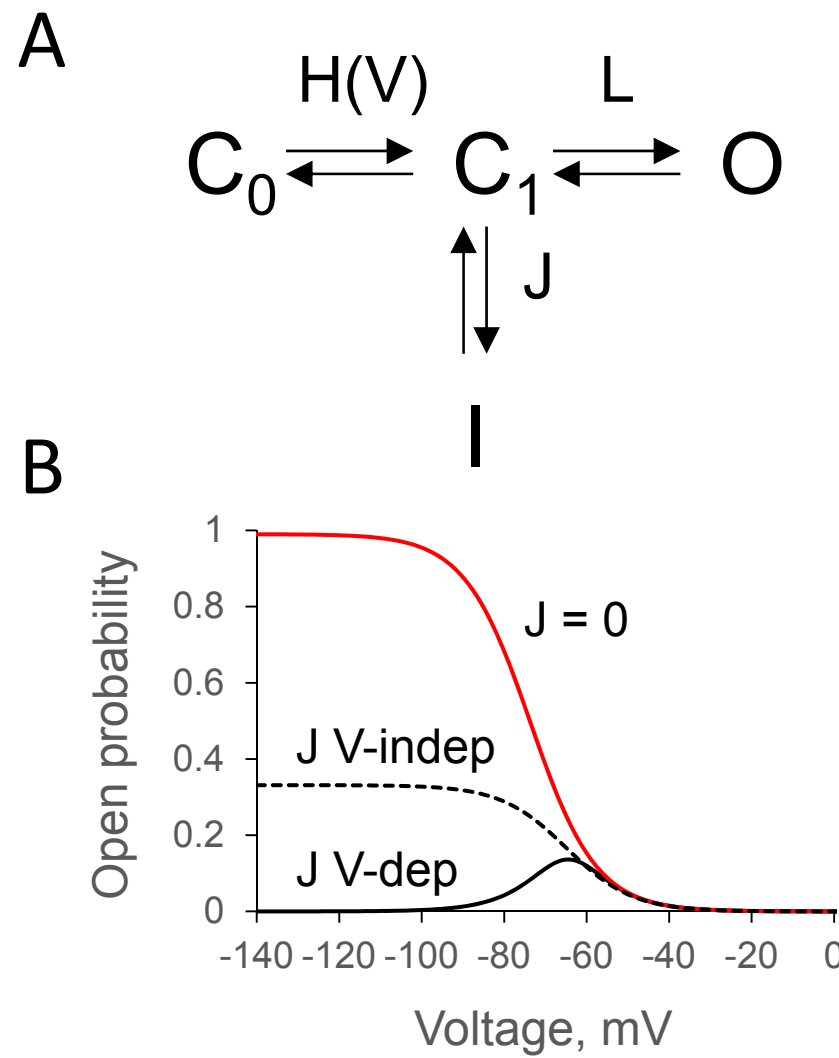


Fig. S5

